Thruster Plume and Spacecraft Interaction Analysis by 3D Electrostatic Code for Hall Thruster

IEPC-2019-858

Presented at the 36th International Electric Propulsion Conference
University of Vienna • Vienna, Austria
September 15-20, 2019

Yasutaka Inanaga[1] and Takanobu Muranaka[2]
[1]*Mitsubishi Electric Corporation, Amagasaki, Hyogo, 661-8661, Japan*
[2]*Chukyo University, Nagoya, Aichi, 466-8666, Japan*

Abstract: We present the development of a 3D electrostatic code to design for large-scale GEO satellites with hall thruster. The electric potential distribution is obtained by Particle-In-Cell, the effects of ion bombardment are computed by Particle Tracking and the deposition by the sputtered particles is accumulated with averaged differential sputtering yield. The accuracy of the code is shown by comparing with the experiment data for SPT-140 hall thruster. Erosion and deposition have been illustrated for the medium scale telecommunication satellite.

Nomenclature

D	=	*deposition rate*	ds	=	*surface area occupied by a computational node*
E	=	*sputtering rate*	e	=	*element charge*
j_p	=	*current density caused by a super particle*	m_i	=	*ion mass*
$\mathbf{n}$	=	*normal vector to surface element*	n_0	=	*reference electron density in Boltzmann relation*
n_b	=	*beam ion density*	n_{CEX}	=	*charge exchange ion density*
n_e	=	*electron density*	n_n	=	*neutral density*
$\bar{S}$	=	*normalized differential sputtering yield*	T_e	=	*electron temperature*
v_i	=	*ion velocity*	Y	=	*sputtering yield (m^3/C)*
α	=	*polar angle measured from surface normal*	β	=	*incident angle measured from surface normal*
ε	=	*incident particle energy*	$\varepsilon*$	=	*sputtering threshold energy*
ε_0	=	*permittivity of vacuum*	θ	=	*beam divergence angle*
σ_{CEX}	=	*cross section of charge exchange*	ϕ	=	*electric potential*
ϕ_{ref}	=	reference *potential in Boltzmann relation*	*suffix* $_{a/s}$	=	*attach/source indicator in deposition calculation*
ψ	=	*azimuthal angle in referring surface measured from incident direction*			

I.Introduction

Hall thruster system has opened an era of being adopted for not only station keeping (SK) but also orbit raising (EOR) for GEO satellites. Some of the ions of the hall thruster plumes could impinge onto a satellite itself and modification to the surface materials. It could cause the mechanical, optical and electrical degradation of the material that is related to the reliability for spacecraft lifetime. Many engineering numerical codes have been developed correspondingly to assess these adverse effects on the satellite design[1~7]

In Japan, the first EOR engineering test satellite, ETS-9, which mounts SPT-type hall thrusters[8] will be launched in FY 2021. Plume analysis should be well-performed in satellite designing phase to ensure the normal operation until EOL and to determine the configuration of the satellite through evaluating these effects. One of major concerns is

[1] Chief Researcher, Advanced Technology R&D Center, Inanaga.Yasutaka@ak.MitsubishiElectric.co.jp.
[2] Associated Professor, Electrical and Electronic Engineering, muranaka@sist.chukyo-u.ac.jp.

surface erosion due to the ion sputtering. In addition, deposition is caused by a part of sputtered particles, scattered toward another surfaces of the satellite structures.

We have been developing a numerical tool applying the numerical technique that had previously been developed in three-dimensional electrostatic plasma simulations[9,10]. The code is designed to achieve for engineering use within the acceptable computation time on commercial workstation. The consistency of the code results to ground experiments and in flight properties is achieved the modeling based on the laboratory experiment data. In our previous work[11], we had presented fundamental algorithm, numerical scheme, modeling of the hall thruster plume for SPT-100, and estimation of the impingement torque for a Russian telecommunication satellite, Express-A. In this paper, calculation result for SPT-140, additional and updated functions, especially deposition on satellite surface by sputtered particles are presented.

II.Numerical Modeling and Algorithm

A. Computation Procedure

In the physical modeling, considered particles in a plume are electrons, beam ions, charge-exchange (CEX) ions, and neutral particles. Fig. 1 (a) indicates the flowchart of the Particle-In-Cell (PIC) simulation to obtain the electric potential distribution. Fig. 1 (b) shows the flow of the Particle Tracking (PT) simulation to evaluate the sputtering of satellite surfaces. Fig. 1 (c) gives the scheme of the calculation of the deposition. In the numerical domain, three-dimensional Cartesian coordinate with the cubic grid system of same spacing is adopted. The numerical modeling to compute the interactions is as follows:

1) Determine the initial spatial distributions of ion beam and neutral gas emitted from a thruster under assumptions of their steady state. The motion of neutral gas is integrated by non-collision particle method. The motion of ion beam is integrated by PIC method self-consistently considered only singly charged beam ion.
2) Electrons are treated as a fluid obeying Boltzmann relationship with uniform electron temperature.
3) The motion of CEX ions, injected into each cell proportional to the beam ion and neutral densities and CEX collision cross section, is integrated by PIC method.
4) The steady state potential distribution with beam and CEX ions is obtained.
5) The effects to spacecraft from both beam and CEX ions are calculated by PT method. Trajectories of test particles colliding onto the surface of satellite are calculated under static electric field. Both singly and doubly charged beam ions are considered. The quantities of these effects, such as sputtering rate are calculated accumulating each contribution of all test particles collided onto surface.
6) The deposition is accumulated with the differential sputtering yield form each sputtered grid.

B. Neutral Gas

The neutral gas is assumed to be emitted with a thermal velocity correspond with the wall temperature of the thruster and with the divergence of $\cos^2\theta$ distribution. The number density corresponding with the backpressure at room temperature add uniformly to the spatial distribution of the neutral gas.

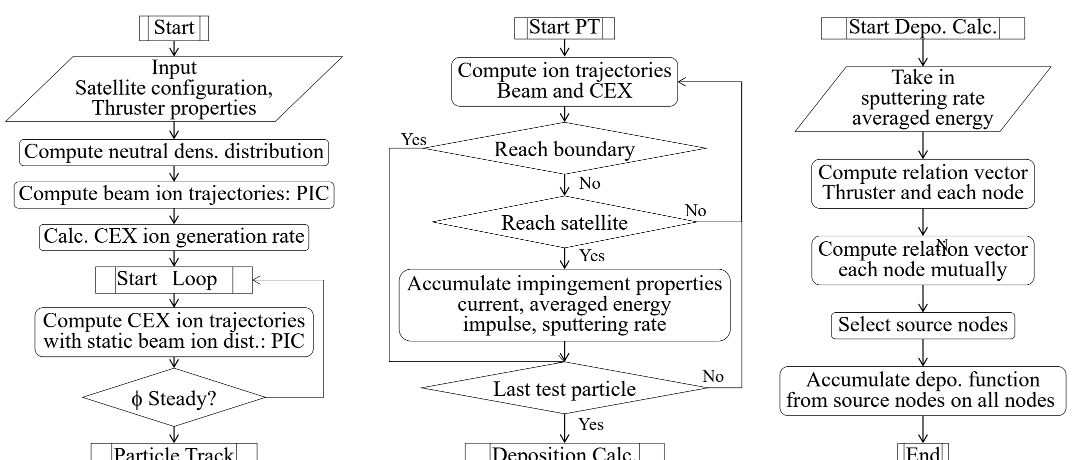

Figure 1. Flowchart of the numerical simulation
(a) main loop with PIC method, (b) PT loop for ion impingement, (c) deposition calculation.

C. Beam Ion

We determined the spatial and velocity distributions of beam ion as follows. The spatial distribution was simply determined to be uniform on the concentric circular area of the thruster exit. The velocity distribution is determined by both the energy and the current distribution measured experimentally result of the ground test. The energy distribution function is described as a function of the beam divergent angle, θ. In addition, we consider that the beam ions have an isotropic temperature that is on the order of the wall temperature of the discharge chamber, so the ions also have the velocity that is determined by an isotropic Maxwellian in three dimensions as well as the beam velocity. Meanwhile, the angular current distribution function is determined by the linear combination of cosine distributions fitting to the experimental result.

D. Charge Exchange Ion

We assumed that the charge exchange ion consisted of only a singly ionized ion that is produced in the plume by charge exchange between the ion beam and the neutral gas. The production rate of CEX ion at a position x is computed locally by (1) at each numerical grid[12].

$$\frac{dn_{CEX}}{dt} = n_n n_i \sigma_{CEX} \qquad (1)$$

The produced CEX ions have a velocity determined by a Maxwellian distribution function of neutral particles. Meanwhile, CEX ions are accelerated outward by plume electric potential, Trajectories of CEX ions are computed by PIC method imposed with the beam ion density distribution pre-calculated.

E. Electron and electric potential

We assume that the distribution of the electrons has the Boltzmann's approximation as described in (2)

$$n_e = n_0 exp\left(\frac{\phi(x)-\phi_{ref}}{T_e}\right) \qquad (2)$$

The electric potential is calculated by the governing equation is a non-linear Poisson's equation described in (3)

$$\triangle\, \phi(x) = \frac{e}{\epsilon_0}\left[n_0 exp\left(\frac{\phi(x)-\phi_{ref}}{T_e}\right) - n_b(x) - n_{CEX}(x)\right] \qquad (3)$$

In PIC method, the charged particles considered are singly charged ion. We iteratively solve the equation (3) using three-dimensional successive over-relaxation (SOR) method. We adopt the Neumann-type boundary condition for the outer boundary, and all potential on and in the spacecraft are able to set any parametric value on each object.

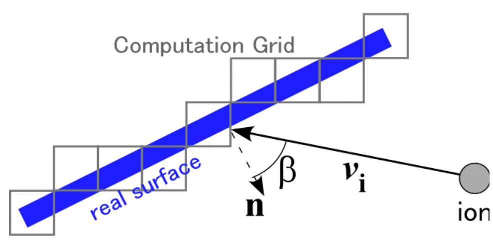

Figure 2. Numerical grid structure with the correction for the real surface.

F. Sputtering Rate

Under the steady state of the electric potential obtained from the PIC routine, collisions of charged particles onto a spacecraft surface is computed by PT method. Both singly and doubly charged beam ions and monovalent CEX ions are considered in this calculation: current, momentum transfer from particles to surface, collision energy and incident angle to the surface. The initial energy of the doubly charged ions was assumed twice as high as by that of the singly ions.

We used the sputtering yield by the ion bombardment and the incident angular dependency from the TRIM[13] calculation. Adjusting the surface energy in TRIM, we forced to fit the presumed yield function in the high energy region to the values of Yamamura's experimental formula[14,15] and the previous experimental result.

We modeled the inner objects by the cubic cell as shown in Fig. 2. To compensate the difference of incident angle in the computational model from the real shape of the component of the satellite, each cell has surface property, which indicate the real surface shown blue line in Fig. 2. The judgements of the ion collision

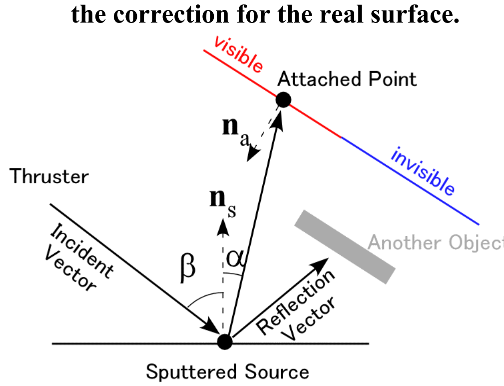

Figure 3. Schematic diagram and angular definition for calculating deposition

onto surface are decided by the virtual cubic boundary, but the incident angles are calculated from real surface. The sputtering rate at each grid position is calculated by following,

$$E_s = \sum^{N} j_p Y(\varepsilon, \beta) \qquad (4)$$

where N is the number of all test particles colliding onto referring surface.

G. Deposition

We did not choose the particle method to compute the deposition. We adopted the accumulation from the differential sputtering yield function to lighten the computational load. The normalized differential sputtering yield function we adopted is Zhang's expression[16, 17],

$$\bar{S}(\alpha,\psi) = C(\beta,\varepsilon)\cdot cos(\alpha)\left[1-\frac{1}{4}\sqrt{\frac{\varepsilon^*}{\varepsilon}}\left(cos(\beta)\,\gamma(\alpha)+\frac{3}{2}\pi sin\,(\beta\,)sin\,(\alpha)cos(\psi)\right)\right] \qquad (5)$$

$$\gamma(\alpha) = \frac{3sin^2(\alpha)-1}{sin^2(\alpha)} + \frac{cos^2(\alpha)(3sin^2(\alpha)+1)}{2sin^3(\alpha)}\, ln\left(\frac{1+sin(\alpha)}{1-sin(\alpha)}\right)$$

where C is the normalized constant depending on the ion incident angle and the energy. Integration of $\bar{S}$ over hemisphere with α, ψ are to be 1 adjusting C. The ion incident angle are calculated by two way. A. In case of the grid point visible from thruster exit center, the incident angle β are calculated directly by the sputtered point - thruster vector (Incident vector in Fig. 3), B. in case of the source point invisible from thruster the incident angle is assumed the normal direction because the collision particles would be mainly CEX ion and the electric field is normal to the plasma contacting surface. ε was adopted the averaged energy weighted by sputtering rate in the PT part. We accumulated the deposition rate at all grid on the satellite surfaces except the invisible points from sputtered source points in following formula,.

$$D_a = \sum^{N_s} \frac{1}{2\pi r_{as}^2}\bar{S}\cdot E_s ds \qquad (6)$$

where N_s is the number of all sputtered source points, r_{as} is the distance from the source to the attached point.

III.Simulation of SPT-140 Ground Test

We evaluated the validity of this plume code by comparing with the ground test result of SPT-140 thruster. Parameters of the thruster, the simulation setting and conditions are shown in Table I and Fig. 4. The electron temperature of 1.5 eV was adopted referring the result from hall thruster plume of SPT-100[18]. This mode is 3 kW of the thruster input power, supposing the station keeping mode. The sampling band to collect the current numerically is determined along the circular line with 30 mm width of 1.0 m radius from the center of the thruster exit.

Figure 5 shows the comparison of current density between the numerical result and the plume ions obtained by the ground test[19]. The back pressure is 2.9×10^{-3} Pa. It is reasonable agreement with the results of ground testing. Figure 6 shows the calculated angular energy distribution. We fitted to the experimental energy distribution[20] by Lorentz function as shown in Fig. 6,

$$E(\theta) = b_0 + \frac{b_1}{\theta^2+b_2} \qquad (5)$$

where $b_{0\sim2}$ are the fitting parameter. We calculated once the sputtering rate for quartz and compared with the experimental rate of the cover glass. The numerical result reduced by order of magnitude in order in the large divergence angular region, then we added the skirt distribution as shown with the red solid line in Fig. 6. Figure 7 shows the sputtering rate of cover glasses at 1 m depart from the thruster exit with SPT-140 ground test[21]. And it is shown the calculation result of the sputtering rate for

TABLE I
Calculation Parameters

Spatial grid width	25 mm
Temporal width (beam / cex)	6.0×10^{-7} / 4.9×10^{-6} s
Calc. step (beam / cex)	3200 / 4519 steps
Thruster potential	0 V
Electron temp.	1.5 eV
Neutral and CEX ion temp.	0.1 eV

SPT-140 hall thruster properties[19]

Thrust	192 mN
Specific Impulse	1683 s
Flow rate (inc. cathode)	11.6 mg/s
Thruster diameter (o./i.)	140/100 mm
Discharge voltage	300 V
Discharge current	10 A
Beam current	7.5 A
Ratio of doubly charged ion curr.	14 %

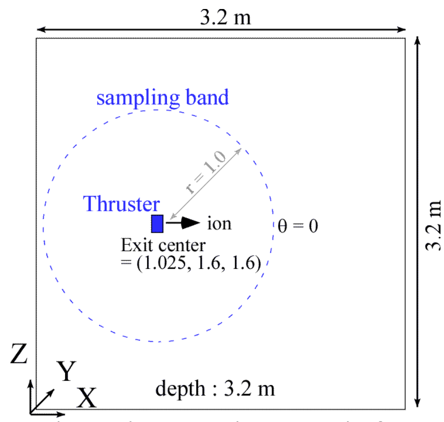

Figure 4. Numerical domain for the simulation of SPT-100 ground test.

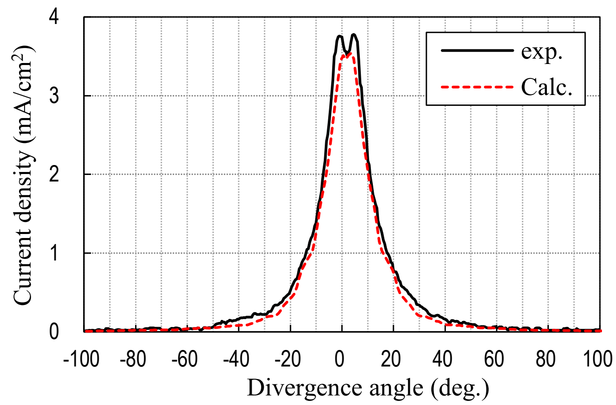

Figure 5. Comparison of current density between the experimental result and calculation.

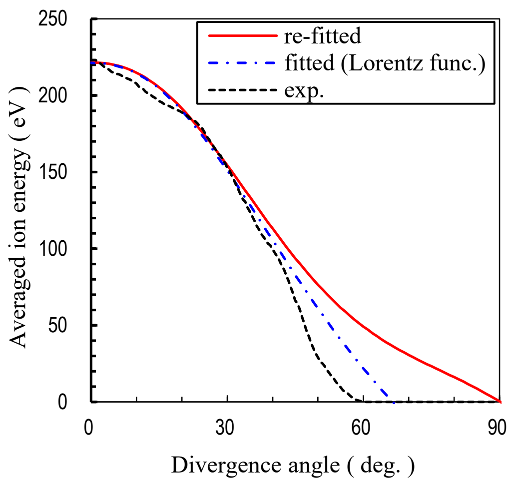

Figure 6. Ion energy dependency on divergence angle.

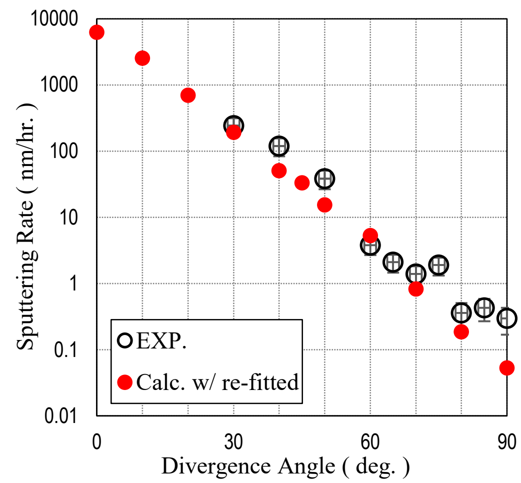

Figure 7. Comparison of sputtering rate between the ground test result and calculation.

quartz with the re-fitted energy distribution function shown in Fig. 6. These shows good agreement of the calculation to experimental data.

IV.Sputtering and Re-deposition Estimation of Express A2

We introduce the numerical estimation of the medium-scale GEO satellite. We focus on the surface erosion and deposition which are of importance for spacecraft design. The estimation was performed for the Russian Express-A satellite that used SPT-100 hall thrusters for North-South station keeping. Fig. 8 shows the drawing of Express[22]. Express-A has the body of 4.1 m high and has four SAPs whose area is about 1.8 × 6.0 m for each. The SPT-100 hall thrusters are mounted on almost middle of the body the X-axis points toward the Earth, the Y-axis points westward, and the Z-axis points northward. The SAP angle was defined as the rotation angle of the SAP that was measured clockwise around the boom along the Z-axis[23]. For the numerical simulation, we employed a numerical model of Express-A,

Figure 8. Picture of the Express spacecraft [15].

TABLE II

Parameters for Express with SPT-100 Thruster[18]

Computational Domain	12 X 4.2 X 5 m (semi wing)
Thrust	85 mN
Specific Impulse	1610 s
Flow rate	5.54 mg/s
Thruster diameter (o./i.)	100/69 mm
Discharge voltage	300 V
Discharge current	4.5 A
Beam current	3.27 A
Ratio of doubly charged ion curr.	20 %
Temporal width (beam / cex)	5.3×10^{-7} / 4.3×10^{-6} s
Calc. step (beam / cex)	10100 / 7363 steps

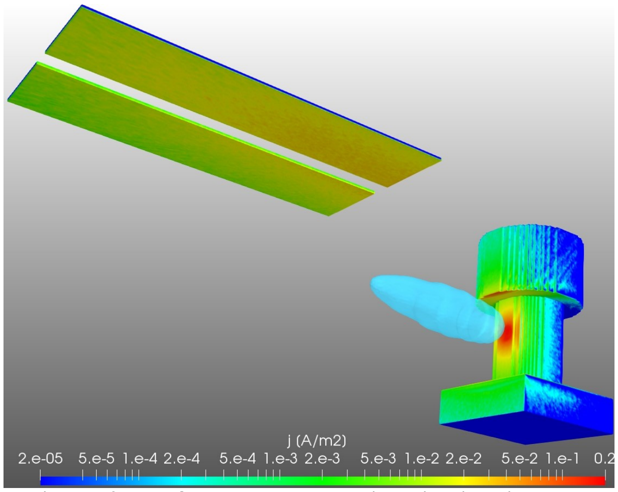

Figure 9. In-flux current density distribution and plume plasma contour ($n_i = 4x10^{14}\ m^{-3}$).

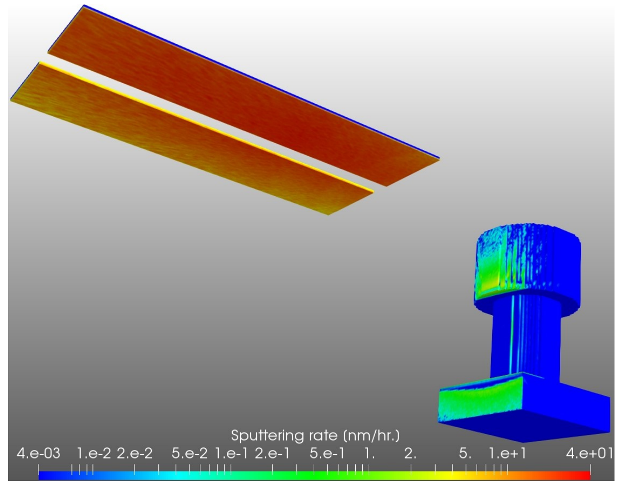

Figure 10. Sputtering rate in case that all the surface is quartz.

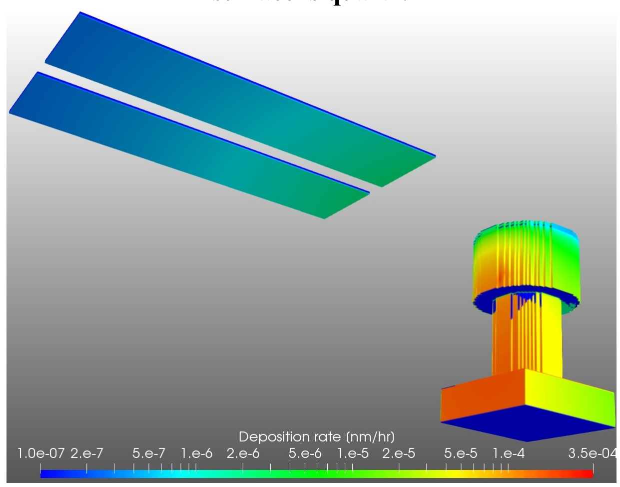

Figure 11. Deposition in case that all the sputtered surface is quartz

which consisted of the body and one-side of the SAP. The SAP was located so that its surface vector was the same direction to that of the top surface of the body.

Figure 9 shows the in-flux current density and the plume plasma shape of the Express-A satellite with a SAP angle of 270 deg. Figure 10 shows the sputtering rate obtained by the numerical simulation on the spacecraft surface for quartz. We included 20%[24] of doubly charged ions as current in the ion beam as well as single Xe ions to estimate sputtering rate. We adopted a model of the uniform surface material, an example is quartz; the material of the cover glass on the SAP. The maximum sputtering rate for quartz was estimated about 40 nm/hr. Meanwhile, we can recognize the current density of the CEX ions on the surface of the body near the thruster whose maximum value is about 170 mA/m^2 in Fig. 9, the sputtering rate in this region is less than $4x10^{-3}$ mm/hr. because the CEX ions have low energy below the threshold value of the quartz sputtering.

The deposition rate in Fig. 11 is remarkable on the satellite body. It is caused by the back scattering particle of the sputtering of the SAP. The maximum deposition rate for quartz, however, is very small estimated below $4x10^{-4}$ nm/hr. comparing from the sputtering rate. This result shows the deposition effects slightly to the satellite performance in this case. In the result mentioned above, we used the real threshold energy and averaged collision energy weighting by the sputtering rate as the energy dependent term in the formula (5): $\sqrt{\varepsilon * / \varepsilon}$. In the literature[17], the measurement results were not fitted for the Zhang's expression using the real threshold energy in Mo, They recommended the value of the energy dependent term was 0.71 at the collision energy of 250 eV in the contrast with the real value of 0.43 and the higher value was needed to matched in the lower collision energy. Therefore we also estimated using the constant energy dependent term of 0.75. The deposition was a little larger than that in Fig. 11. In any case, an experimental verification of deposition rate will be necessary.

V.Conclusion

We have developed a 3D electrostatic code to analyze the effect to spacecraft by hall thruster plume. The code adopted a simplified algorithm for engineering use within acceptable calculation time on a commercial workstation by the combination of PIC and PT methods to compute the trajectories of ions and the plume potential.

We presented a model of beam profile of SPT-140 hall thruster to adjust the angular distributions of the current density and energy to the experiment data, which showed reasonable agreement with the experiment in the angular distributions of current densities and sputtering ground test result.

Then, we made the numerical estimation of the surface erosion due to the ion bombardment and the deposition by the sputtered particles for Russian Express-A satellite. We could conclude the deposition did not significantly affect the satellite performance, while the sputtering rate was high value in this system.

In this code, we hypothesized the uniform electron temperature model. This might cause the under estimation of the potential around thruster exit and the reduction of the CEX ion back flow. The improvement of this issue is the future work. We will apply to the satellite design practically while extending the functions and improving the accuracy of this code.

References

[1]T. Randolph, E. Pencil, and D. Manzella, "Far-Field Plume Contamination and Sputtering of the Stationary Plasma Thruster," Proc. 30th Joint Propulsion Conference, Indianapolis, 1994, AIAA-94-2855.

[2]D. Allison, J. Baldwin, and M. Scharfe, "Development of BEPPA: An Object-Oriented Particle Code for Full 3-D Spacecraft Plume Analysis and Satellite Design," Proc. 44th Joint Propulsion Conference & Exhibit, Hartford, 2008, AIAA-2008-4999.

[3]R. Corey, and D. Pidgeon, "Electric Propulsion at Space Systems/Loral," Proc. 31st International Electric Propulsion Conference, Ann Arbor, 2009, IEPC-2009-270.

[4]I.G. Mikellides, G.A. Jogeward, B.M. Gardner, I. Katz, M.J. Mandell and V.A. Davis, "A Hall-Effect Thruster Plume and Spacecraft Interactions Modeling Package," Proc. 27th International Electric Propulsion Conference, Pasadena, 2001, IEPC-01-251.

[5]I.G. Mikellides, M. J. Mandell, R.A. Kuharski, D.A. Davis, B. M. Gardnert, and J. Minor, "The Electric Propulsion Interactions Code (EPIC): A Member of the NASA Space Environment and Effects Program (SEE) Toolset," Proc. 39th Joint Propulsion Conference and Exhibit, Huntsville, 2003, AIAA-2003-4871.

[6]I.G. Mikellides, I. Katz, H. Kamhawi, and J. L. Vannoord, "Numerical Simulations of a 20-kW Class Hall Thruster Using the Magnetic-Field-Aligned-Mesh Code Hall2De," Proc. 32nd International Electric Propulsion Conference, Wiesbaden, 2011, IEPC-2011-244.

[7]L. Brieda and M. Keidar," Multiscale Modeling of Hall Thrusters," Proc. 32nd International Electric Propulsion Conference, Wiesbaden, 2011, IEPC-2011-101.

[8]I. Funaki, S. Cho, T. Sano, T. Fukatsu, Y. Tashiro, T. Shiiki, and Y. Nakamura, "Hall Thruster Breadboard Model Development for ETS-9," Proc. 32nd Int. Symp. Sp. Technol. Sci., 2019, ISTS-2019–b-003.

[9]T. Muranaka, H. Hosoda, J. Kim, S. Hatta, K. Ikeda, T. Hamanaga, M. Cho, H. Usui, H. O. Ueda, K. Koga, and T. Goka, "Development of Multi-Utility Spacecraft Charging Analysis Tool (MUSCAT)," IEEE Trans. on Plasma Sci., vol. 36, no. 5, pp. 2336-2349, 2008.

[10]T. Muranaka, I. Shinohara, I. Funaki, Y. Kajimura, M. Nakano, and R. Takaki, "Research and Development of Plasma Simulation Tools in JEDI/JAXA," J. Space Tech. Sci., vol. 25, no. 2, pp. 1-18, 2011.

[11]T. Muranaka and Y. Inanaga, "Development of a Numerical Tool for Hall Thruster Plume and Spacecraft Interaction Analysis," Trans. JSASS, Aerospace Tech. Japan, Vol. 16, No. 5, pp. 366-373, 2018.

[12]J. Wang, D. Brinza, and M. Young, "Three-Dimensional Particle Simulations of Ion Propulsion Plasma Environment for Deep Space 1," J. Spacecraft and Rockets, vol. 38, no.3, pp. 433-440, 2001.

[13]http://www.srim.org/ (accessed May 19th, 2019).

[14]Y. Yamamura, and H. Tawara, "Energy Dependence of ion-Induced Sputtering Yields from Monoatomic Solids at Normal Incidence," Atomic Data and Nuclear Data Tables, vol. 62, pp.149-253, 1996.

[15]Y. Yamamura, Y. Itikawa, N. Itoh, "Angular dependence of sputtering yields of monatomic solids," IPPJ-AM-26, 1983.

[16]Zhang, Z.L., Zhang, L., "Anisotropic Angular Distributions of Sputtered Atoms," Radiation Effects and Defects in Solids, Vol. 159, 2004, pp. 301-307.

[17]Yalin, A. P., Williams, J. D., Surla, V., Wolf, J., and Zoerb, K. A., "Azimuthal Differential Sputter Yields of Molybdenum by Low Energy Ion Bombardment," 42nd AIAA Joint Propulsion Conference (Sacramento, CA), 2006, AIAA paper 2006-4335.

[18]D. Manzella and J. Sankovic, "Hall Thruster Beam Characterization,"Proc. 31st Joint Propulsion Conference and Exhibit, San Diego, 1995, AIAA-95-2927.

[19]Hargus, W. Jr., Fije, J. M., Mason, L., Jankovsky, R., Haag, T., Pinero, I. and Synder, J. S.: "Preliminary Performance Results of the High Performance Hall System SPT-140," Proc. 36th JPC, AIAA-2000-3250, 2000.

[20]Kozubsky, K., Kudriavtzev, S. and Pridannikov, S.: "Plume Study of Multimode Thruster SPT-140," Proc. 26th International Electric Propulsion Conference, Kitakyushu, 1999, IEPC-99-073, 1999.

[21]Fije, J. M., Hargus, W. Jr., Jaworske, D. A., Sarmiento, C., Mason, L., Jankovsky, R., Synder, J. S., Malone, S., Haas, J. and Gallimore, A.: "Spacecraft Interaction Test Results of the High Performance Hall System SPT-140," Proc. 36th JPC, AIAA-2000-3521, 2000.

[22]http://space.skyrocket.de/doc_sdat/ekspress-a.htm (accessed May 20th, 2018).

[23]N. Sitnikova, D. Volkov, I. Maximov, V. Petrusevich, and D. Allen, "Hall Effect Thruster Interactions Data From the Russian Express-A2 and Express-A3 Satellites," NASA/CR-2003-212005/PART1.

[24]I. Katz, R. R. Hofer, and D. M. Goebel, "Ion Current in Hall Thrusters," Proc. 30th International Electric Propulsion Conference, Florence, Italy, 2007, IEPC-2007-365.